Research Square

Preprints are preliminary reports that have not undergone peer review.
They should not be considered conclusive, used to inform clinical practice,
or referenced by the media as validated information.

# Pancreatic Lineage Cell Differentiation of Bone Marrow Mesenchymal Stromal Cells on Acellular Pancreatic Bioscaffold

**Zhao Li**
Peking University People's Hospital
**Yue Du**
Tianjin Medical University
**Xin Wang** ( wx007146@163.com )
Nankai University Affiliated Hospital https://orcid.org/0000-0002-6416-953X

**Research**

**Keywords:** pancreas, acellular pancreatic bioscaffold, bone mesenchymal stromal cells, proliferation, differentiation, chronic pancreatitis

**Posted Date:** October 23rd, 2020

**DOI:** https://doi.org/10.21203/rs.3.rs-59795/v2

**License:** This work is licensed under a Creative Commons Attribution 4.0 International License.
Read Full License

# Abstract

**Background:**We evaluated(1) the potential differentiation ability of bone mesenchymal stromal cells(BMSCs) into pancreatic lineage cells on rat acellular pancreatic bioscaffold (APB) and (2) the effect of differentiated BMSCs on chronic pancreatitis in vivo.

**Methods:**After BMSCs were isolated and characterized, they were dynamically cultured on APB and statically cultured in tissue culture flasks (TCFs), with or without growth factor(GF) in both culture systems. We assessed cytological behavior, such as the proliferation and differentiation of BMSCs, by morphological observation, flow cytometry, enzyme-linked immunosorbent assay (ELISA), quantitative real-time/reverse transcriptase polymerase chain reaction, and Western blot analysis. For the in vivo study, we evaluated the pancreatic fibrosis and pathological scores.We detected the expression of α-SMA,collagen types I and III,and IL-10 in pancreatic tissue by ELISA.

**Results:**The most appropriate flow rate for the dynamic culture of BMSCs was 4mL/min. The proliferation rates of BMSCs in the APB groups were significantly higher than in the TCF groups.During the pancreatic lineage cell differentiation process, APB induced BMSCs to express mRNA markers such as PDX-1 and PTF-1 at higher levels. In contrast, the marker Oct4 was expressed at a lower level in the APB group.  All tested pancreatic cytokeratins, including α-Amy, CK7, Flk-1, and C-peptide, were expressed at higher levels in the APB group. The secretion of metabolic enzymes, such as Amy and insulin, was higher in the APB system. By scanning electron microscopy and transmission electron microscopy, the ultrastructure of BMSCs in the APB group further revealed the morphological characteristics of pancreatic-like cells. In the in vivo study, the expression of α-SMA and collagen types I and III in tissues was significantly lower in differentiated BMSCs group, whereas the levels of IL-10 in pancreatic tissue were higher in differentiated BMSCs with significant difference. In addition, in both the in vitro and the in vivo study, GF significantly improved proliferation, differentiation, and pancreatic cell therapy.

**Conclusion:** Our data showed (1) the capacity of APB, a three-dimensional pancreatic biomatrix, to promote BMSC differentiation toward pancreatic lineage and pancreatic-like phenotypes, and (2) the considerable potential of using these cells for pancreatic cell therapies and tissue engineering.


# Introduction

Severe pancreatic diseases, such as severe acute pancreatitis and pancreatic cancer, may cause pancreatic failure, which poses a serious harm to human health, with an increasingly high global mortality rate[1-4]. Because effective therapies are lacking, pancreas transplantation has been proposed as a potential therapeutic alternative for the treatment of organ defects or tissue injury. Organ transplantation is greatly limited by the imbalance between demand and supply of suitable donor organs[5]; thus, regenerative medicine (RM), as an interdisciplinary and attractive field of research, has sought to overcome the limitations of replacement and transplantation treatment by facilitating the natural development of tissue[6].

One of the roadblocks to success in the RM field is the identification of cells that can be used to regenerate bioengineered organs[7-8]. Stem cells and their descendants or committed progenitors are capable of proliferating and differentiating into specialized cells[9]. Because of their ability to self-renew and indefinitely maintain a population with identical properties through symmetric and asymmetric cell divisions, stem cell therapies for diseased solid organs are an important potential modality of RM[10].

Mesenchymal stem cells (MSCs) can be isolated from tissues such as bone marrow, adipose tissue, umbilical cord tissue, and amniotic fluid. Because of their characteristics such as self-renewal and multilineage differentiation capability into osteogenic, adipogenic, chondrogenic, and myogenic- and neurogenic-like lineages[11-15], MSCs offer great therapeutic potential and have been developed to treat a wide range of disorders.

The most extensively studied MSCs are bone mesenchymal stromal cells (BMSCs), characterized as fibroblast-like cells, which are isolated from bone marrow mesenchymal cellular populations. BMSCs are renowned in RM for their multilineage differentiation potential and easy acquisition[15,16]. Aside from their remarkable proliferative and multilineage differentiation and regenerative potential, BMSCs can affect the surrounding microenvironment by their multiple paracrine functions[17,18]. Also, they have immunomodulatory and antioxidant properties[19]. Since the introduction of cell therapy as a strategy for the treatment of many diseases, BMSCs have emerged as ideal candidates.

BMSCs can differentiate into cells of pancreatic lineages under certain culture conditions[20]. But such inducing strategy cannot provide conditions for BMSCs to proliferate rapidly with high viability. Also, these kinds of induced BMSCs do not maturely express all important pancreatic-lineage cell markers. Moreover, they exhibit a loss of stem cell characteristics and functions after expansion in vitro[21,22].

Acellular matrix (ACM) can serve as an ideal three-dimensional (3D) platform for regenerative medicine because it is biocompatible and preserves a 3D geometric and spatial architecture[23]. ACM has physiological levels of biochemical components, matrix-bound growth factors (GFs) , and cytokines[24]. Furthermore, ACM has intact and patent vasculature structures that could transport nutrition and oxygen for seeding cells to attach and localize to specific topographical positions[25].

A previous study indicated that certain kinds of whole-organ ACM could support BMSCs to differentiate into mature cells and express functional markers[26-29]. Furthermore, this type of induced cells has potential applications in regenerative therapy and tissue repair[30]. Little is known, however, about the stimulatory effects of whole-organ ACM on BMSC differentiation into pancreatic lineage cells.

Past work from our laboratory indicated the biological utility of acellular pancreatic bioscaffold (APB) as whole-organ ACM, which could support and enhance the proliferation and differentiation of AR42J pancreatic acinar cells for regenerative medicine[31]. Therefore, in this study, we investigated the ability of APB to promote BMSC proliferation and differentiation, which may improve regenerative therapy.

# Materials And Methods

## Isolation and identification of BMSCs

All animal work was approved by the Institutional Animal Care of China and performed in accordance with the Animal Welfare Act Institutional Guidelines. We collected BMSCs from the bone marrow of adult Sprague–Dawley rats (weighing approximately 250 g, between 6 and 7 weeks old). The rats were killed using chloroform, and the femur and tibia were removed. To collect BMSCs, a 23-gauge syringe was inserted into the bone cavity and flushed with serum-free Dulbecco's modified Eagle's medium (DMEM). After centrifuging at 1200 rpm for 10 min, the bone marrow cells were resuspended in DMEM (HyClone, Logan UT, USA) that was supplemented with 10% fetal bovine serum (FBS), 10 U/mL penicillin, 10 μg/mL streptomycin (Gibco, Australia), and 1% L-glutamate (Sigma-Aldrich, St. Louis, MO, USA). Finally, the number of viable cells was checked and transferred to culture dishes at a density of $5\times10^5$ cells per $cm^2$ in high-glucose DMEM containing 10% FBS for incubation at 37°C and a 5% $CO_2$ atmosphere. The medium was changed every 2 to 3 days. Only low-passage (≤5) cells were used in experiments. Cells were passaged every 7–10 days at a 1:3 ratio. BMSCs were characterized by flow cytometry for detection of CD90, CD29, and CD45 expression.

## Decellularization of rat pancreas and reseeding of APB

Adult Sprague–Dawley rats weighing approximately 250 g, ages 6 to 7 weeks, were killed. As previously described, the pancreata were decellularized by Easy-Load Digital Drive peristaltic pumps and the biocompatibility of APB was assessed[31,32]. BMSCs were reseeded onto APB and cultured in the biomimetic bioreactor system made by our laboratory for 7 days to evaluate repopulation and further differentiation. Cells were seeded on APB by multistep infusion with $2.5\times10^6$ cells in 2 mL each through the hepatic portal vein and the pancreatic duct. Medium was changed every 2–3 days. We observed the ultrastructure of seeded BMSCs on APB by scanning electron microscopy (SEM) and transmission electron microscopy (TEM). Additionally, to assay the optimal flow rate of APB supporting the proliferation of BMSCs, the dynamic culture was perfused retrogradely at different speeds (0, 0.5, 1, 2, 4, and 6 mL/min). We quantified the DNA content of BMSCs in the APB scaffold at each speed on days 4 and 7.

## Analysis of BMSC characteristics by laser scanning confocal microscopy (LSCM)

Tissue samples were fixed in 4% formaldehyde (ThermoFisher, Waltham, MA, USA), cryo-protected with 30% sucrose, and cut into 5 μm thick sections. For immunostaining, we used rabbit primary antibodies (1:200; Boersen, China). We used goat antirabbit Alexa Fluor 488 (1:500; Invitrogen, Carlsbad, CA, USA) as a secondary antibody. For co-labeling using antibodies from the same host species, we conducted sequential staining by GFP (BioHermes, USA). After the first primary antibody staining, we included an additional blocking step before adding a secondary antibody. The slides were washed three times with 1× PBS (5–10 min each) before being mounted with ProLong Gold Anti-fade Reagent with DAPI (Invitrogen). After washing, the cells were incubated with streptavidin-conjugated Texas red (Tx-R) for 30 min at 37°C,

washed six times (10 min each) with PBS, and mounted on glass slides using FITC-guard (Testog Inc., IL, USA) as the mounting medium.

We then examined cells in a PHOIBOS 1000 laser scanning confocal microscope (Sarastro, Stockholm, Sweden). Tx-R was excited with an argon laser. We collected and used the emitted signals to create 3D reconstructions of serial confocal sections using the program Vanis (Sarastro).

### In vitro differentiation of BMSCs into pancreatic lineage cells

After BMSCs were reseeded on APB for 7 days, they were induced into pancreatic-like clusters in differentiation culture systems (i.e., dynamic culture on the APB and static culture in TCFs) in three steps for another 21 days. We recorded the time at the end of day 7 of BMSCs reseeding on APB as time zero.

Step 1: BMSCs were cultured in high-glucose DMEM (25 mM) containing 2% FBS, 0.2 mM β-mercaptoethanol (Gibco), 10 ng/mL bFGF (Peprotech, USA), and 10 ng/mL EGF (Peprotech) for 7 days.

Step 2: BMSCs were cultured in serum-free high-glucose DMEM (25 mM) containing 10 ng/mL bFGF, 10 ng/mL EGF, 2% B27 (Gibco), 0.5% BSA, 10 mM nicotinamide (Sigma), and 10 ng/ml exendin-4 (Sigma) for 7 days.

Step 3: The cells were cultured in serum-free high-glucose DMEM (25 mM) containing 10 ng/mL EGF, 10 ng/mL Activin A (Peprotech), 10 ng/mL betacellulin (Peprotech), 2% B27, and 0.5% BSA for 7 days. The medium was changed every 2 days.

In the static culture system, cells were cultured in the TCF system with zero flow rate, while in the APB dynamic system, cells were cultured in the biomimetic bioreactor system on APB at the optimal flow speed. Depending on whether the differentiation was induced by GF in the culture system, we divided our study into four groups: BMSCs cultured in TCFs without GF (TCF-GF(-)), BMSCs cultured in TCFs with GF (TCF-GF(+)), BMSCs cultured on APB without GF (APB-GF(-)), and BMSCs cultured on APB with GF (APB-GF(+)).

### Analysis of the morphological characteristics of differentiating BMSCs by SEM and TEM

The samples were fixed in 2.5% glutaraldehyde in 0.1 M PBS (pH 7.4) for 60 min and washed thoroughly three times with 0.1 M PBS for 15 min each. Next, the samples were fixed in 1% $OsO_4$ in 0.1 M PBS for 60 min. This was followed by three more PBS washing steps for 15 min each. The samples were then dehydrated in gradient series of alcohol for 15 min each. Additionally, samples were critical point dried and coated with Au/Pd using a Cressington Coater 108A sputter coater. We took electron microscope images using a JEOL JSM-6335F field emission SEM.

For TEM, the samples were fixed in 2.5% glutaraldehyde in PBS, post-fixed in 1% $OsO_4$ in PBS, dehydrated through a graded series of alcohols, and embedded in Epon. We cut thin (60 nm) sections using a Reichert Ultracut S, mounted on 200 mesh copper grids, and counterstained with 2% aqueous

uranylacetate for 7 min and 1% aqueous lead citrate for 2 min. We observed the samples with a JEOL 1011 TEM.

### Cell proliferation assay

We analyzed bromodeoxyuridine (BrdU) incorporation immunohistochemically using a BrdU immunohistochemistry system. We assessed cell proliferation by measuring BrdU incorporation using a commercially available BrdU enzyme-linked immunosorbent assay (ELISA) kit (Abcam, Cambridge, UK) according to the manufacturer's protocol. Cells were fixed with fixation solution and incubated with anti-BrdU antibody for 90 min. After washing, we added tetramethyl-benzidine and measured absorbance by a spectrophotometric plate reader at 405 nm.

### Assessment of the expression of pancreatic lineage gene markers by real-time/reverse transcriptasepolymerase chainreaction

We extracted RNA using a NucleoSpin kit (Seebio Biotech, China) according to the manufacturer's protocol. We measured the absorbance at 280 and 260 nm using a BioRad Smart Spec spectrophotometer (Biorad Laboratories, Hercules, CA, USA) to evaluate the RNA concentration and quality. We performed reverse transcription using the ImProm II (Promega, Madison, WI, USA) reverse transcription kit according to the manufacturer's recommendations. We performed quantitative real-time polymerase chain reaction analysis for pancreatic acinar genes. Experiments were repeated in triplicate.

### Quantification of pancreatic functional cytokeratins by western blot

We prepared whole-cell lysates to evaluate important pancreatic proteins. We used antibodies at the following concentrations: anti-α-amylase (α-Amy), 1:1000; anti-cytokeratin 7 (CK7), 1:2500; anti-C-peptide, 1:2500; and anti-fetal liver kinase-1 (Flk-1), 1:2000. Membranes were incubated with the appropriate HRP-conjugated secondary antibody (1:5000). Antibody binding was detected by chemiluminescence radiography. Membranes were scanned, recorded digitally, and processed using ImageJ software.

### Quantification of potential metabolic function of differentiated BMSCs in vitro

For the insulin release assay in vitro, we treated cell clusters using four different glucose concentrations (5, 10, 15, and 25 mM). The samples were pre-incubated with Krebs–Ringer bicarbonate (KRB) buffer for 1 h. Subsequently, the clusters were removed and incubated for 1 h in KRB buffer containing different concentrations of glucose. The supernatant was collected and frozen at −80°C. We measured insulin levels using a rat insulin ELISA kit (Mercodia, Sweden) according to the manufacturer's protocol.

We measured Amy secretion according to four different cholecystokinin (CCK) concentrations: 0, $10^{-9}$, $10^{-8}$, and $10^{-7}$ mM. The Amy levels are expressed as ratios between the amount of Amy released into the extracellular medium and the total cellular Amy, as determined by permeabilizing cells with 0.1% SDS in 10 mM phosphate buffer (pH 7.8). Amy levels were spectrophotometrically measured using the Phadeba

amylase kit according to the manufacturer's protocol. We performed both processes at the end of the differentiation process.

### In vivo studies of differentiated BMSCs

To investigate the possibility to use differentiated BMSCs to treat chronic pancreatitis (CP) in vivo, we randomly divided the rates into six groups ($n$ = 10 rats per group): (1) the control group, (2) the model group, and (3–6) four treatment groups (BMSCs cultured with TCF-GF(-), TCF-GF(+), APB-GF(-), and APB-GF(+)). The CP rat model was induced by infusion of dibutyltin dichloride (DBTC) through the caudal vein. For the treatment group, $3\times10^6$ differentiated BMSCs in 1 mL were injected through the caudal vein on days 20, 27, and 34 after model induction. For the model group, an equal volume of saline was injected into the caudal vein.

We collected pancreatic tissues 80 days after model induction for histopathological examination and detected the expression of alpha-smooth muscle actin (α-SMA), collagen types I and III, and interleukin-10 (IL-10) by ELISA.

### Immunofluorescence staining of fibrotic markers

Tissue samples were fixed in 4% formaldehyde, cryoprotected with 30% sucrose, and cut into 5 μm thick sections. For immunostaining, we used the following rabbit primary antibodies: anti-α-SMA, anti-collagen type I, anti-collagen type III, and anti-IL-10 (1:200). We used goat anti-rabbit Alexa Fluor 488 (1:500) as a secondary antibody. For co-labeling using antibodies from the same host species, we conducted sequential staining. After the first primary antibody staining, an additional blocking step was included before we added a secondary antibody. The slides were washed three times with 1× PBS (5–10 min each) before being mounted with ProLong® Gold Anti-fade Reagent with DAPI. We recorded images with MetaMorph 7.5.6.0 on an Olympus microscope.

### Statistical analysis

Data are expressed as mean (standard deviation). Significant differences among groups were determined by the Student $t$-test for two-group comparisons and analysis of variance of repeated measure followed by post hoc analysis for multiple-group comparisons. Probability values at $P < 0.05$ indicated statistical significance.

## Results

### Characterization of BMSCs isolated from bone marrow

BMSCs in Passage 1 exhibited an irregular round shape and size (Figure 1a), whereas in Passage 3 they changed to a regular form and had a spindle fibroblast-like appearance (Figure 1b). Of early-passage BMSCs (between passage 2 and 4), 90.21% were positive for both CD90 and CD29, 98.53% were positive for CD90 and negative for CD45, and 93.38% were positive for CD29 and negative for CD45.

### Repopulation of APB with BMSCs in pancreatic bioreactor cultures

The seeded BMSCs attached on the surface of the APB bioscaffold and exhibited different shapes(yellow arrows). We observed the adhesion among neighboring cells(white arrows) by SEM(Figure 2a). Also, LSCM indicated that BMSCs not only attached to the surface of the bioscaffold but also formed in clusters along the inner structure of the APB. The 3D scaffolds reseeded with the GFP-positive cells(green) were counterstained with component collagen(red) and DAPI(blue)(Figure 2b). The APB,as the 3D scaffolds, could support the reseeding of BMSCs.

Also, the DNA quantification of the BMSC-APB graft showed that 4mL/min for the dynamic culture system was the optimal flow rate for BMSC proliferation on both day 4 and day 7, with a significant difference compared with other flow speeds ($P$<0.05) (Figure3).

### The ultrastructural characteristics of BMSCs during differentiation

SEM analysis revealed that undifferentiated BMSCs exhibited a spindle fibroblast-like appearance with little microvilli at the cell surface(Figure 4a). We did not observe any mature organelles by TEM(Figure 4b,4c).

SEM analysis revealed that differentiated BMSCs at day 21 were spherical in shape with more dense microvilli at the cell surface(Figure 5a).There was a major increase in the number of epithelial-like cell clusters(white arrow; Figure 5b) with a complex intercalation of the extracellular matrix(ECM)(black arrow; Figure 5b). Differentiating endocrine and exocrine cells developed from the BMSCs and subsequently formed isolated small clusters(Figure 5c). A significant amount of ECM fibers accumulated around each newly differentiated cell as well as the cell clusters(Figure 5d).

By TEM, we observed that pancreatic-like epithelial cells(white arrow)were organized into ductal structures(black arrow) surrounded by scattered individual mesenchymal-like stellate cells (Figure 5e). The epithelial cells had formed small clusters separate from the ducts(black arrow; Figure 5f).Acinar cells increased in number and formed amylase/Amy-positive cell clusters(red arrow;Figure 5f). The cell clusters for insulin also increased in numbers and formed islet-like structures (white arrows; Figure 5f) that contained capillaries (yellow arrows; Figure 5f).

Also, TEM showed glycogen positivity in ductal cells (black arrows), nuclei (blue arrows),secretory granules(yellow arrow), mitochondria(white arrow),and smooth and rough endoplasmic reticulum(red arrow) in differentiated BMSCs(Figure 5g).

### BMSC proliferation during differentiation

To determine whether the APB allowed BMSCs to grow and to compare its efficacy with other culture systems(Figure 6),we performed a BrdU incorporation assay to analyze time-dependent growth of BMSCs from days 3 to 21.From day3,the cell proliferation rate was significantly higher in the APB dynamic system than in the TCF culture whether with or without GF($P$<0.05).Also,in the presence of GF, the

proliferation rate was higher in both the APB system and the TCF system, with a significant difference from day3($P$<0.05).These results suggest that the APB efficiently facilitated pancreatic-like cell growth and that GF promoted BMSC proliferation.

### Evaluation of the gene expression of pancreatic markers

To assess the ability of the APB to support BMSC differentiation, we assessed the expression of pancreatic genes at different time points (Figure 7). PDX-1 and PTF-1 gene expression increased, whereas Oct4 expression decreased from day 3 to day 21 in all groups. Furthermore, in both culture systems, expression of PDX-1and PTF-1was higher,whereas Oct4 expression was lower in the GF(+) groups compared with the GF(-) groups. In addition, whether with or without GF, the expression of PDX-1and PTF-1 was higher whereas the expression of Oct4 was lower in BMSCs cells cultured on theAPB. The expression of PDX-1 and PTF-1was higher in APB-GF(-) cells than in TCF-GF(-) cells with a significant difference from day 7($P$<0.05),and it was higher in APB-GF(+) cells than in TCF-GF(+) cells with a significant difference from day 3($P$<0.05). Conversely, Oct4 expression was lower in APB-GF(-) cells than in TCF-GF(-) cells with a significant difference from day 5 ($P$<0.05), but it was lower in APB-GF(+) cells than in TCF-GF(+) cells,with a significant difference from day 3 ($P$<0.05).

### Evaluation of the expression of pancreatic cytokeratins

To verify these findings, we performed western blotting of pancreatic cytokeratins (Figure 8).The protein expression of α-Amy, CK7, C-peptide, and Flk-1 increased from day 3 to day 21 in all groups. Also, in both culture systems, the expression of all four cytokeratins was higher in GF(+) groups compared with GF(-) groups. In addition, with or without GF, the expression of the four cytokeratins was higher in BMSCs cultured on the APB than in BMSCs in the TCF group. The expression of C-peptide was higher in APB-GF(-) cells than in TCF-GF(-) cells,with a significant difference from day 5 ($P$<0.05), and it was higher in APB-GF(+) cells than in TCF-GF(+) cells, with a significant difference from day 3($P$<0.05). The expression of the other three cytokeratins was higher in APB-GF(-) cells than in TCF-GF(-) cells, with a significant difference from day 14($P$<0.05), but it was higher in APB-GF(+) cells than in TCF-GF(+) cells with a significant difference from day 5($P$<0.05). The gene and cytokeratin results suggested that pancreatic cell differentiation was enhanced in the presence of APB and that GF promoted BMSC differentiation.

### Assessment of differentiated BMSCs

We detected insulin secretion levels(pg) of the cell clusters in the presence of 5,10,15,and 25mM glucose(Figure9a). The insulin levels were enhanced when concentrations of glucose increased in all four groups. At the lowest concentration(5mM), there was no significant difference among the four groups($P$>0.05). At a concentration of 10mM, in the presence of GF, there was a significant difference between the dynamic and the static system($P$<0.05). In both systems, however, there was no significant difference between the presence or absence of GF($P$>0.05). At glucose concentrations of 15 and 25mM, whether with or without GF, insulin secretion levels were higher in the APB groups than in the TCF

groups($P$<0.05), and the levels of insulin were significantly higher in the presence of GF in both APB and TCF culture systems ($P$<0.05).

We detected α-Amy secretion levels in the culture systems in the presence of $10^{-11}$,$10^{-10}$,$10^{-9}$, and $10^{-8}$ mM CCK(Figure 9b). The Amy levels were enhanced with increasing CCK concentrations in all four groups. At a concentration of $10^{-11}$ or $10^{-10}$ mM, we did not find any significant difference among the four groups($P$>0.05). At a concentration of $10^{-9}$ or $10^{-8}$ mM, we observed significant differences in α-Amy secretion levels between the APB system and the TCF system whether with or without GF($P$<0.05) and between the presence and absence of GF in both culture systems ($P$<0.05).

### CP treatment with differentiated BMSC in vivo

Both the pathological score and the pancreatic fibrosis score(Table 1) were lower in each treatment group compared with the model group($P$<0.05).In the four treatment groups,with or without GF,the pathological score and the pancreatic fibrosis score were lower in the APB group than in the TCF group($P$<0.05). In addition,in both culture systems,the scores were higher in the GF(-) groups than in GF(+) groups($P$<0.05).

The tissue expression levels of α-SMA, collagen types I and III(Table 2) were lower in each treatment group than in the model group($P$<0.05),whereas the levels of IL-10 in pancreatic tissue were higher in the treatment groups than in the model group($P$<0.05).In the four treatment groups, with or without GF, the expression levels of α-SMA and collagen types I and III were lower, but the levels of IL-10 were higher in the APB group than in the TCFgroup($P$<0.05). In addition, in both culture systems, the expression levels of α-SMA and collagen types I and III were lower,but the levels of IL-10 were higher in the GF(+) groups than in the GF(-) groups($P$<0.05).

We also investigated the expression of fibrotic markers(α-SMA, collagen types I and III, IL-10) in tissues by immunofluorescence(Figure 10). The levels of all three fibrotic markers were lower in all treatment groups, but the levels of IL-10 were higher, than in the model group. In the four treatment groups, with or without GF, the expression levels of α-SMA and collagen types I and III were lower, but the levels of IL-10 were higher, in the APB group than in the TCF group. In addition, in both culture systems, the expression levels of α-SMA and collagen types I and III were lower, but the levels of IL-10 were higher, in the GF(+) groups than in the GF(-) groups.

# Discussion

For both in vivo and in vitro tissue regeneration, it is essential for the donor cell to have the following characteristics: (1) the ability to differentiate into pancreatic cell types, (2) high proliferative potential (ability to expand to high numbers before seeding onto the APB), (3) easy accessibility (an autologous cell source, either differentiated or stem), and (4) lack of immunogenicity. These characteristics point to the possibility of using BMSCs as a source for reseeding on APB or as in vivo cell therapy.

The growth of cells is regulated by their microenvironment, including the attachment among cells and the presence of signaling molecules. It is important for cells to proliferate and differentiate in a culture system mimicking the microenvironment of their innate tissue, which cannot be accomplished by traditional two-dimensional culture systems [33,34]. ACM, with a preserved complex multifaceted ECM composition, 3D spatial orientation, and microstructure, has a tissue-specific biological nature as well as biocompatible properties that can promote cell adhesion, viability, proliferation, and differentiation[35]. Also, ACM has physiological levels of GFs, such as insulin-like GF, bone morphogenetic protein 4, and cytokines, for regeneration and implantation[36,37]. This may explain why APBs have the ability to promote BMSC differentiation.

Furthermore, dynamic culture with an appropriate flow rate is better for BMSC proliferation and differentiation than static culture in APB. Dynamic culture benefits the delivery of $O_2$ and nutrients, and metabolic waste can be easily removed in flow culture systems[38]. In addition, the flow speed in the dynamic culture system can generate a liquid shearing force, which can appropriately modulate BMSC proliferation and differentiation. Lowering or enhancing the flow rate affects the proportion of apoptotic BMSCs[39]. At a flow rate of 4 mL/min, BMSCs could survive and proliferate with high viability in the dynamic culture system. Therefore, we used a flow rate of 4 mL/min in our study.

In our study, BMSCs could be reseeded to repopulate the surface and the center of APB, as indicated by morphological assessment.

For the purpose of BMSC differentiation, we added GF in both culture systems. During the differentiation process, BMSCs proliferated in all four groups. The cell proliferation rate was higher in the APB (dynamic) system than in the TCF (static) culture system. The proliferation rate was higher in the APB-GF(+) system than in the APB-GF(-) system. These results indicated that the APB efficiently facilitated pancreatic-like cell growth and GF promoted BMSC proliferation during differentiation.

With respect to ultrastructural characteristics of BMSCs during differentiation, the shape of cells changed to spherical, and cells exhibited more dense microvilli. Both endocrine and exocrine cells increased in number and formed epithelial cell-like clusters, with significant amounts of accumulated ECM fibers. In addition, our study clearly showed glycogen positivity, nuclei, secretory granules, and mature organelles such as mitochondria and smooth and rough endoplasmic reticulum. This indicated that BMSCs differentiated into pancreatic-like cells. A previous study has indicated that cell aggregation is a necessary condition for BMSC differentiation[40]. This result was in accordance with our current research.

To assess pancreatic differentiation, we evaluated the gene expression of PDX-1 and PTF-1, which are known to be important to pancreatic function. PDX-1 plays a vital role in pancreatic development and differentiation[41]. PTF-1, as a transcriptional regulator of exocrine-specific genes and an exocrine transcription factor, is responsible for pancreatic exocrine function and exocrine gene expression[42]. In our research, without GF, PDX-1 and PTF-1 expression was higher on the APB system than on the TCF

system with a significant difference from day 7, and with GF, the difference was statistically significant from day 3. This indicated that APB supported BMSC differentiation and GF increased the function of APB.

In contrast, the expression of Oct4, a pluripotency marker associated with the differentiation potential of BMSCs[43], decreased after differentiation. Oct4 expression was lower in cells cultured on the APB system than in cells cultured on the TCF system with a significant difference after day 5 without GF, and with a significant difference from day 3 with GF. The gene expression of PDX-1, PTF-1, and Oct4 indicated that APB promoted BMSC differentiation, reducing their pluripotency capacities, into pancreatic-like cells, especially with the help of GF.

To identify the pancreatic-like cells, we assessed the expression of cytokeratins such as α-Amy, CK7, C-peptide, and Flk-1. α-Amy is a well-established marker of pancreatic acinar cells. Both CK7 and Flk-1 are localized normally in the pancreatic duct structures in the adult pancreas and contribute to the formation of the large intralobular, interlobular, and main ducts[44]. Coupled with CK7, Flk-1 functions as the receptor of vascular endothelial growth factor, which is associated with the endothelial layer of the vasculature[45,46]. These two markers are known to be expressed during pancreatic morphogenesis in the fetus[47]. C-peptide is expressed in pancreatic endocrine cells, which indicates β-cells function[48].

Our study indicated that the expression of α-Amy, CK7, and Flk-1 was significantly higher in BMSCs cells cultured on the APB than in the TCF group after day 14 without GF, but it was higher from day 5 with GF. Also, C-peptide levels were higher in cells cultured on the APB system than in TCF cells after day 5 without GF and from day 3 with GF. The cytokeratin results suggested that BMSCs differentiated into two major pancreatic lineage cell types: (1) endocrine cells, which were arranged mainly in groups as islets of Langerhans and secrete different polypeptides delivered to other parts of the body via the vasculature; and (2) acinar exocrine cells, whose secretions were carried away through the ductal system. Thus, GF strengthened the stimulatory effects of APB on BMSCs.

Research has indicated that the mechanical characteristics, such as the stiffness and biomechanical strength, of ACM are related to BMSC differentiation through TGF-β. Also, the changing ECM density inhibits capillary morphogenesis and neovascularization in vivo in a manner consistent with that observed in vitro[49,50]. This may be another mechanism mediating the inductive effects of the APB.

We also assessed the metabolic function of differentiated BMSCs. To demonstrate the endocrine function, we compared the insulin secretion levels at different glucose concentrations. The insulin levels were enhanced when glucose concentrations increased. Insulin secretion levels were significantly higher in the APB groups than in TCF groups at glucose concentrations of 15 and 25 mM. GF could significantly increase insulin secretion. Such a trend was not significant at low glucose concentrations.

Similarly, the α-Amy levels were enhanced when concentrations of CCK increased. At CCK concentrations of $10^{-9}$ and $10^{-8}$ mM, α-Amy levels were significantly higher in the APB system than in the TCF system. α-Amy secretion significantly increased in the presence of GF. Low levels of CCK did not follow such a

trend. Previous studies indicated that CCK at less than $10^{-8}$ mM could stimulate Amy secretion in a concentration-dependent manner, whereas CCK at higher concentrations might inhibit Amy secretion[51]. We utilized less than $10^{-8}$ mM CCK in our study.

The assay of metabolic function indicated that APB with GF promoted the pancreatic organogenesis of BMSCs and supported BMSC differentiation into primary functional units, which maintained their respective phenotypic expression (endocrine β-cells: insulin; exocrine acinar cells: Amy) — in proximity to their respective native niches.

As whole-organ ACM physiologically resembles the original tissue, including intact 3D architecture, preserved native ECM components, vascular networks, and biomechanical properties, it could guide tissue regrowth and encourage cell differentiation when combined with biological agents[52]. Our study was in agreement with this previous study,

Another previous study has indicated that BMSCs are less immunogenic for they do not express MHC class II markers and do not elicit a strong immune response, as evidenced by a lack of activation of T cells[53]. Additionally, BMSCs are easily acquired and easily accessible. On the basis of these merits of BMSCs, our findings supported in vivo cell therapy efforts, as well as in vitro treatments in whole pancreas regeneration.

A pathological hallmark of CP is progressive fibrosis, which is mediated by pancreatic stellate cells (PSCs). One of the earliest cellular events at the initiation of fibrosis is activation of PSCs, which can be mediated concomitantly by a variety of factors, such as oxidative stress, cytokines, and GFs. The process of PSC activation involves significant expression of α-SMA, which can promote the secretion of collagen types I and III[54,55]. IL-10 has been indicated to be a protective cytokine and has been shown to decrease the severity of chronic pancreatitis and to reduce the likelihood of systemic complications. Also, it can downregulate collagen synthesis in both unstimulated and activated PSCs[56,57].

Our study indicated that the expression of α-SMA and collagen types I and III could be downregulated, whereas the expression of IL-10 could be upregulated in differentiated BMSCs in vivo. This indicated that differentiated BMSCs inhibited the process of fibrosis after transplantation in vivo and exerted protective effects on pancreatic tissue.

Note that this study had several unavoidable limitations. First, after BMSC differentiation, the cells did not have intact phenotypic properties and functions of native pancreatic cells. We plan to improve our differentiation strategy in further research. Second, this study was based on an animal model. In future studies, we will aim to provide insights regarding the feasibility and usefulness of bioscaffolds and cells in humans. Third, our study focused on APB and BMSCs in vitro. Efforts to improve pancreatic tissue engineering in vivo will be made in future research.

Despite these limitations, we believe that our data on the effects of APB on BMSCs are valuable and reliable.

# Conclusions

APB supported the proliferation and viability of BMSCs in a dynamic culture system with an optimal flow rate of 4 mL/min. During the differentiation process, APB could (1) induce BMSC differentiation into pancreatic-like cells which express gene markers and pancreatic functional cytokeratins and (2) promote secretion of metabolic enzymes. GF could significantly improve proliferation, differentiation, and cell engraftment in APB. Our study sheds light on the possibilities to develop pancreatic cell therapies and improve pancreatic tissue engineering.

# Abbreviations

BMSC: bone mesenchymal stromal cell

MSC: mesenchymal stem cell

APB: acellular pancreatic bioscaffold

ACM: acellular matrix

CP: chronic pancreatitis

TCF: tissue culture flask

GF: growth factor

SEM: scanning electron microscopy

TEM: transmission electron microscopy

LSCM: laser scanning confocal microscopy

PDX: pancreatic duodenal homeodomain containing transcription factor

PTF: pancreatic exocrine transcription factor

Oct: octamer-binding transcription factor

α-Amy: α-amylase

CK7: cytokeratin 7

Flk-1: fetal liver kinase-1

ECM: extracellular matrix

CCK: cholecystokinin

BMSC: bone mesenchymal stromal cell

MSC: mesenchymal stem cell

APB: acellular pancreatic bioscaffold

ACM: acellular matrix

CP: chronic pancreatitis

TCF: tissue culture flask

GF: growth factor

SEM: scanning electron microscopy

TEM: transmission electron microscopy

LSCM: laser scanning confocal microscopy

PDX: pancreatic duodenal homeodomain containing transcription factor

PTF: pancreatic exocrine transcription factor

Oct: octamer-binding transcription factor

α-Amy: α-amylase

CK7: cytokeratin 7

Flk-1: fetal liver kinase-1

ECM: extracellular matrix

CCK: cholecystokinin

# Declarations

**Ethics approval and consent to participate:** All animal work was approved by the Institutional Animal Care of China and performed in accordance with the Animal Welfare Act Institutional Guidelines.

**Consent for publication:** Not applicable.

**Availability of data and materials:** Data sharing not applicable to this article as no datasets were generated or analyzed during the current study.

**Competing interests:** The authors declare that they have no competing interests.

**Funding:** National Science Foundation (81502509) and National Science Foundation of Tianjin City (2014KY04).

**Conflict-of-interest statement**

There is no conflict of interest to declare.

**Author contributions:** Wang Xin and Li Zhao designed the research; Wang Xin and Du Yue performed the research; Du Yue contributed new reagents and analytic tools; Wang Xin and Li Zhao analyzed the data and wrote the paper.

**Acknowledgments:** The authors thank the Department of Public Health of Tianjin Medical University for the integrity of the data and the accuracy of the data analysis.

**Authors' information:**

**Zhao Li,** Department of Hepatobiliary Surgery, Peking University People's Hospital; Beijing Key Laboratory of Liver Cirrhosis and HCC Basic Research;

**Yue Du,** Department of Public Health, Tianjin Medical University, Tianjin, P.R. China;

**Xin Wang,** Department of General Surgery, The Fourth Center Hospital, Tianjin, China; Division of Bioengineering, Department of Regenerative Medicine, The Fourth Center Hospital, Tianjin, China. Key Laboratory of Hormones and Development (Ministry of Health), Key Laboratory of Metabolic Diseases, Tianjin Metabolic Diseases Hospital. Institute of Endocrinology, Tianjin Medical University, Tianjin, China.

# References

[1] Ibadov RA, Arifjanov AS, Ibragimov SK, et al. Acute respiratory distress-syndrome in the general complications of severe acute pancreatitis. Ann Hepatobiliary Pancreat Surg. 2019;23 (4):359-364.

[2] Zhou X, Wang W, Wang C,et al.DPP4 Inhibitor Attenuates Severe Acute Pancreatitis-Associated Intestinal Inflammation via Nrf2 Signaling. Oxid Med Cell Longev. 2019 Nov 15;2019:6181754.

[3] Wang X, Shan YQ, Tan QQ, et al. MEX3A knockdown inhibits the development of pancreatic ductal adenocarcinoma. Cancer Cell Int. 2020 Feb 28;20:63.

[4] Wenhao Luo, Gang Yang, Wentao Luo, et al. Novel therapeutic strategies and perspectives for metastatic pancreatic cancer: vaccine therapy is more than just a theory. Cancer Cell Int. 2020; 20: 66.

[5] Rijkse E, IJzermans JN, Minnee RC. Machine perfusion in abdominal organ transplantation: Current use in the Netherlands. World J Transplant. 2020;10(1):15-28.

[6] Porzionato A, Stocco E, Barbon S, et al.Tissue Engineered Grafts from Human Decellularized Extracellular Matrices: A Systematic Review and Future Perspectives.Int J Mol Sci. 2018;19(12).

[7] Mendez JJ, Ghaedi M, Steinbacher D, et al. Epithelial cell differentiation of human mesenchymal stromal cells in decellularized lung scaffolds. Tissue Eng Part A. 2014;20(11-12):1735-1746.

[8] Kim IG, Ko J, Lee HR, et al. Mesenchymal cells condensation-inducible mesh scaffolds for cartilage tissue engineering. Biomaterials. 2016;85:18-29.

[9] Junyent S, Garcin CL, Szczerkowski JLA,et al. Specialized cytonemes induce self-organization of stem cells. Proc Natl Acad Sci USA. 2020 Mar 17.

[10] Lanzoni G1, Oikawa T, Wang Y,et al. Concise review: clinical programs of stem cell therapies for liver and pancreas.Stem Cells. 2013;31(10):2047-2060.

[11] Mizuno H, Tobita M, Uysal AC.Concise review: Adipose-derived stem cells as a novel tool for future regenerative medicine.Stem Cells. 2012;30(5):804-810.

[12] Lin HT, Otsu M, Nakauchi H. Stem cell therapy: an exercise in patience and prudence.Philos Trans R Soc Lond B Biol Sci.2013;368(1609):20110334.

[13] Ra JC, Shin IS, Kim SH,et al. Safety of intravenous infusion of human adipose tissue-derived mesenchymal stem cells in animals and humans.Stem Cells Dev. 2011;20(8):1297-1308.

[14] Rastegar F, Shenaq D, Huang J,et al. Mesenchymal stem cells: Molecular characteristics and clinical applications. World J Stem Cells. 2010;2(4):67-80.

[15] Wang Y, Chen X, Cao W,et al.Plasticity of mesenchymal stem cells in immunomodulation: pathological and therapeutic implications. Nat Immunol. 2014;15(11):1009-1016.

[16] Zhou LL, Liu W, Wu YM,et al.Oral Mesenchymal Stem/Progenitor Cells:The Immunomo-dulatory Masters. Stem Cells Int. 2020;2020:1327405.

[17] Fawzy E-Sayed KM, Elahmady M, Adawi Z,et al. The periodontal stem/progenitor cell inflammatory-regenerative cross talk: A new perspective. J Periodontal Res. 2019;54(2):81-94.

[18] C. Brown, C. McKee, S. Bakshi, et al. Mesenchymal stem cells:cell therapy and regeneration potential. Journal of Tissue Engineering and Regenerative Medicine. 2019;13(9): 1738–1755.

[19] Ma Z, Song G, Liu D,et al. N-Acetylcysteine enhances the therapeutic efficacy of bone marrow-derived mesenchymal stem cell transplantation in rats with severe acute pancreatitis. Pancreatology. 2019;19(2):258-265.

[20] Leung PS, Ng KY. Current progress in stem cell research and its potential for islet cell transplantation. Curr Mol Med. 2013;13(1):109-125.

[21] Li M, Zhang T, Jiang J,et al. ECM coating modification generated by optimized decellularization process improves functional behavior of BMSCs.Mater Sci Eng C Mater Biol Appl. 2019;105:110039.

[22] Yin H, Wang Y, Sun Z,et al.Induction of mesenchymal stem cell chondrogenic differentiation and functional cartilage microtissue formation for in vivo cartilage regeneration by cartilage extracellular matrix-derived particles. Acta Biomater. 2016;33:96-109.

[23] Salvatori M, Katari R, Patel T, et al. Extracellular matrix scaffold technology for bioartificial pancreas engineering:state of the art and future challenges.J Diabetes SciTechnol.2014;8(1):159–169.

[24] Tsuchiya T, Balestrini JL, Mendez J, et al. Influence of pH on extracellular matrix presservation during lung decellularization. Tissue Eng Part C Methods.2014;20(12):1028–1036.

[25] Orlando G, Farney AC, Iskandar SS, et al. Production and implantation of renal extracellular matrix scaffolds from porcine kidneys as a platform for renal bioengineering investigations. Ann Surg. 2012;256(2):363–370.

[26] Zhao W, Li J J, Cao D Y, et al. Intravenous injection of mesenchymal stem cells is effective in treating liver fibrosis.World J Gastroenterol,2012,18(10):1048-1058.

[27] Kakabadze A, Mardaleishvili K, Loladze G,et al. Reconstruction of mandibular defects with autogenous bone and decellularized bovine bone grafts with freeze-dried bone marrow stem cell paracrine factors.Oncol Lett. 2017;13(3):1811-1818.

[28] Yin H, Wang Y, Sun Z,et al. Induction of mesenchymal stem cell chondrogenic differentiation and functional cartilage microtissue formation for in vivo cartilage regeneration by cartilage extracellular matrix-derived particles.Acta Biomater.2016;33:96-109.

[29] Santhakumar R,Vidyasekar P,Verma RS. Cardiogel: a nano-matrix scaffold with potential application in cardiac regeneration using mesenchymal stem cells.PLoS One.2014;9(12): e114697.

[30] Li M, Zhang T, Jiang J, et al. ECM coating modification generated by optimized decellularization process improves functional behavior of BMSCs.Mater Sci Eng C Mater Biol Appl. 2019;105:110039.

[31] Wang X, Li YG, Du Y, et al. The Research of Acellular Pancreatic Bioscaffold as a Natural 3-Dimensional Platform In Vitro. Pancreas. 2018;47(8):1040-1049.

[32] Goh SK, Bertera S, Olsen P, et al. Perfusion-decellularized pancreas as a natural 3D scaffold for pancreatic tissue and whole organ engineering.Biomaterials. 2013;34(28):6760–6772.

[33] Gaetani R, Aouad S, Demaddalena LL, et al. Evaluation of different decellularization protocols on the generation of pancreas-derived hydrogels.Tissue Eng Part C Methods.2018 Nov6.

[34] Porzionato A, Stocco E, Barbon S,et al.Tissue-Engineered Grafts from Human Decellularized Extracellular Matrices: A Systematic Review and Future Perspectives.Int J Mol Sci. 2018 Dec 18;19(12).

[35] Ungerleider JL, Johnson TD, Hernandez MJ, et al. Extracellular matrix hydrogel promotes tissue remodeling, arteriogenesis, and perfusion in a rat hindlimb ischemia model. JACC Basic Transl Sci. 2016;1(1-2):32-44.

[36]Crapo P M, Gilbert T W, Badylak S F. An overview of tissue and whole organ decel-lularization processes[J]. Biomaterials,2011,32(12):3233-3243.

[37] Kniazeva E, Kachgal S, Putnam A J. Effects of extracellular matrix density and me-senchymal stem cells on neovascularization in vivo[J]. Tissue Eng Part A, 2011,17(7-8):905-914.

[38] Hwang N S, Varghese S, Elisseeff J. Controlled differentiation of stem cells. Adv Drug Deliv Rev,2008,60(2):199-214.

[39] Cartmell S H, Porter B D, Garcia A J, et al. Effects of medium perfusion rate on cell-seeded three-dimensional bone constructs in vitro. Tissue Eng, 2003,9(6):1197-1203.

[40] Guo Y, Chen S, Xu L,et al. Decellularized and solubilized pancreatic stroma promotes the in vitro proliferation, migration and differentiation of BMSCs into IPCs. Cell Tissue Bank. 2019;20(3):389-401.

[41] Park CH, Lee JY, Kim MY, et al. Oligonol, a low-molecular-weight polyphenol derived from lychee fruit, protects the pancreas from apoptosis and proliferation via oxidative stress in streptozotocin-induced diabetic rats.Food Funct. 2016;7(7):3056–3063.

[42] Barlass U, Dutta R, Cheema H,et al. Morphine worsens the severity and prevents pancreatic regeneration in mouse models of acute pancreatitis. Gut. 2018;67(4):600-602.

[43] Fafián-Labora J, Morente-López M, Sánchez-Dopico MJ,et al. Influence of mesenchymal stem cell-derived extracellular vesicles in vitro and their role in ageing. Stem Cell Res Ther. 2020 Jan 3;11(1):13.

[44] Rooman I, Heremans Y, Heimberg H, et al. Modulation of rat pancreatic acinoductal trans - differentiation and expression of PDX-1 in vitro. Diabetologia. 2000;43(7):907-914.

[45] Di Rocco G, Tritarelli A, Toietta G, et al. Spontaneous myogenic differentiation of Flk-1-positive cells from adult pancreas and other nonmuscle tissues. Am J Physiol Cell Physiol. 2008;294(2):C604–C612.

[46] Dygai AM, Skurikhin EG, Pershina OV, et al. Role of hematopoietic stem cells in inflammation of the pancreas during diabetes mellitus. Bull Exp Biol Med. 2016;160(4):474-479.

[47] Xue A, Julovi SM, Hugh TJ, et al. A patient-derived subrenal capsule xenograft model can predict response to adjuvant therapy for cancers in the head of the pancreas. Pancreatology. 2015;15(4):397-404.

[48] Boughton C, Allen JM, Tauschmann M,et al. Assessing the effect of closed-loop insulin delivery from onset of type 1 diabetes in youth on residual beta-cell function compared to standard insulin therapy (CLOuD study): a randomised parallel study protocol. BMJ Open. 2020;10(3):e033500.

[49] Park J S, Chu J S, Tsou A D, et al. The effect of matrix stiffness on the differentiation of mesenchymal stem cells in response to TGF-beta[J]. Biomaterials. 2011,32(16):3921-3930.

[50] Subramanian K, Owens D J, O'Brien T D, et al. Enhanced differentiation of adult bone marrow-derived stem cells to liver lineage in aggregate culture[J]. Tissue Eng

Part A,2011,17(17-18):2331-2341.

[51] Gukovskaya AS, Gukovsky I, Jung Y, et al. Cholecystokin in induces caspase activation and mitochondrial dysfunction in pancreatic acinar cells. Roles in cell injury processes of pancreatitis. J Biol Chem. 2002;277(25):22595-22604.

[52] Gong T, Heng BC, Lo EC, et al. Current advance and future prospects of tissue engineering approach to dentin/pulp regenerative therapy. Stem Cells. Int. 2016;2016:9204574.

[53] Rasmusson I, Ringdén O, Sundberg B et al. Mesenchymal stem cells inhibit the formation of cytotoxic T lymphocytes, but not activated cytotoxic T lymphocytes or natural killer cells. Transplantation. 2003;76(08):1208-1213.

[54] Ratnakar R Bynigeri, Aparna Jakkampudi, Ramaiah Jangala, et al. Pancreatic Stellate Cell:Pandora's Box for Pancreatic Disease Biology.World J Gastroenterol. 2017;23(3):382-405.

[55] Hannah M Komar, Gregory Serpa, Claire Kerscher, et al. Inhibition of Jak/STAT signaling reduces the activation of pancreatic stellate cells in vitro and limits caerulein-induced chronic pancreatitis in vivo.Sci Rep. 2017;7(1):1787.

[56] Fu-Xiang Yu, Long-Feng Su, Chun-Lei Dai,et al.Inhibition of Pancreatic Stellate Cell Activity by Adipose-Derived Stem Cells. Hepatobiliary Pancreat Dis Int. 2014;14(2):215-221.

[57] Manohar M, Verma AK, Venkateshaiah SU, et al. Pathogenic mechanisms of pancreatitis. World J Gastrointest Pharmacol Ther. 2017; 8(1): 10–25.

# Tables

| Table 1 The pancreatic fibrosis and pathological score | | | |
|---|---|---|---|
| Group | n | pathological score | pancreatic fibrosis score |
| Controlgroup | 10 | 0 | 0 |
| Model group | 10 | 9.89±3.31 | 2.51±0.41 |
| Treatment group | | | |
| TCF-GF(-) | 10 | 7.79±2.57 | 0.96±0.18 |
| TCF-GF(+) | 10 | 5.84±2.11 | 0.78±0.17 |
| APB-GF(-) | 10 | 3.91±1.33 | 0.61±0.24 |
| APB-GF(+) | 10 | 2.11±0.86 | 0.37±0.09 |
| F | | 3.182 | 4.055 |
| P | | 0.038 | 0.024 |

| Table 2 The expression of α-SMA, collagen type I and III, IL-10in pancreatic tissue(mg/ml) | | | | | |
|---|---|---|---|---|---|
| | n | α-SMA | collagen type I | collagen type III | IL-10 |
| Control group | 10 | 70.22±24.41 | 42.59±19.56 | 230.79±85.55 | 2808.11±927.58 |
| Model group | 10 | 168.56±71.25 | 94.37±37.51 | 789.68±293.47 | 3137.68±986.89 |
| Treatment group | | | | | |
| TCF-GF(-) | 10 | 79.65±21.28 | 45.13±15.21 | 263.14±81.52 | 2373.57±721.13 |
| TCF-GF(+) | 10 | 56.45±18.21 | 29.21±10.12 | 136.14±45.23 | 4864.27±2071.41 |
| APB-GF(-) | 10 | 46.52±14.13 | 24.32±8.17 | 131.31±41.34 | 4618.98±1861.12 |
| APB-GF(+) | 10 | 22.15±7.28 | 10.15±3.25 | 73.14±18.25 | 7614.08±2071.41 |
| F | | 4.003 | 5.184 | 3.523 | 5.216 |
| P | | 0.033 | 0.013 | 0.035 | 0.009 |

# Figures

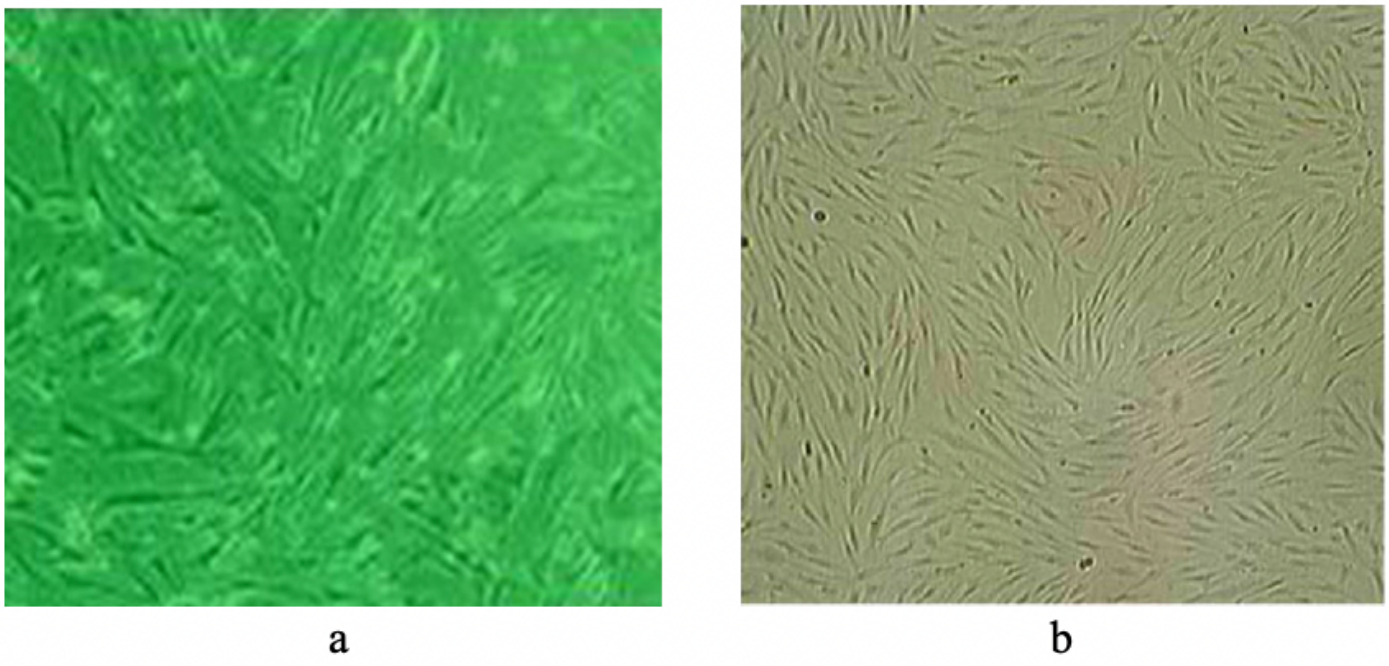


**Figure 1**

The morphology of BMSCs isolated from bone marrow. a)The morphology of BMSCs in Passage 1. b) The morphology of BMSCs in Passage 3.

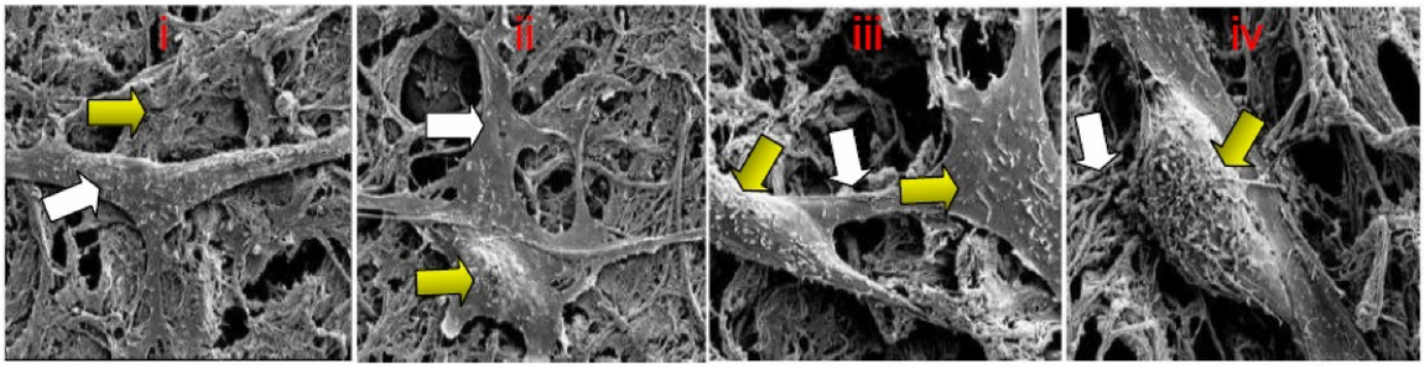


a

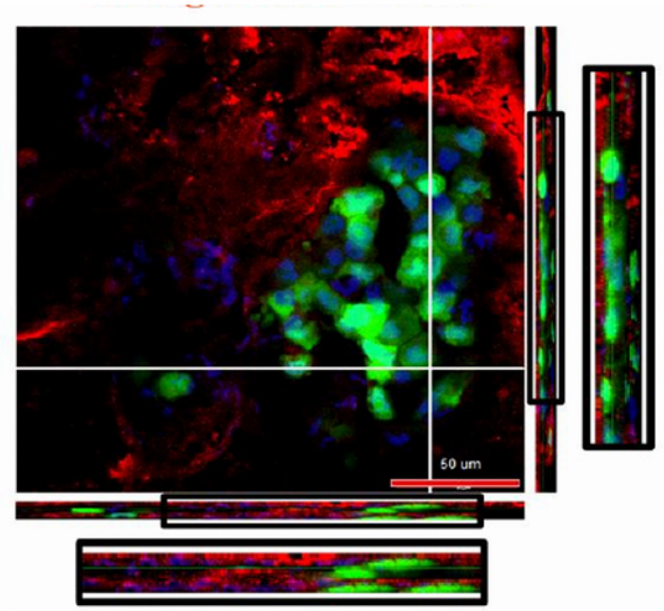


b

## Figure 2

The morphology of BMSCs reseeded on APB by SEM and LSCM a)The seeded BMSCs attached on APB and the adhesion among neighboring cells by SEM(Scale bars=1μm). b)BMSCs not only attached on the surface of the bioscaffold, but also formed in cluster in the inner structure of APB indicated by LSCM (Scale bars=1μm).

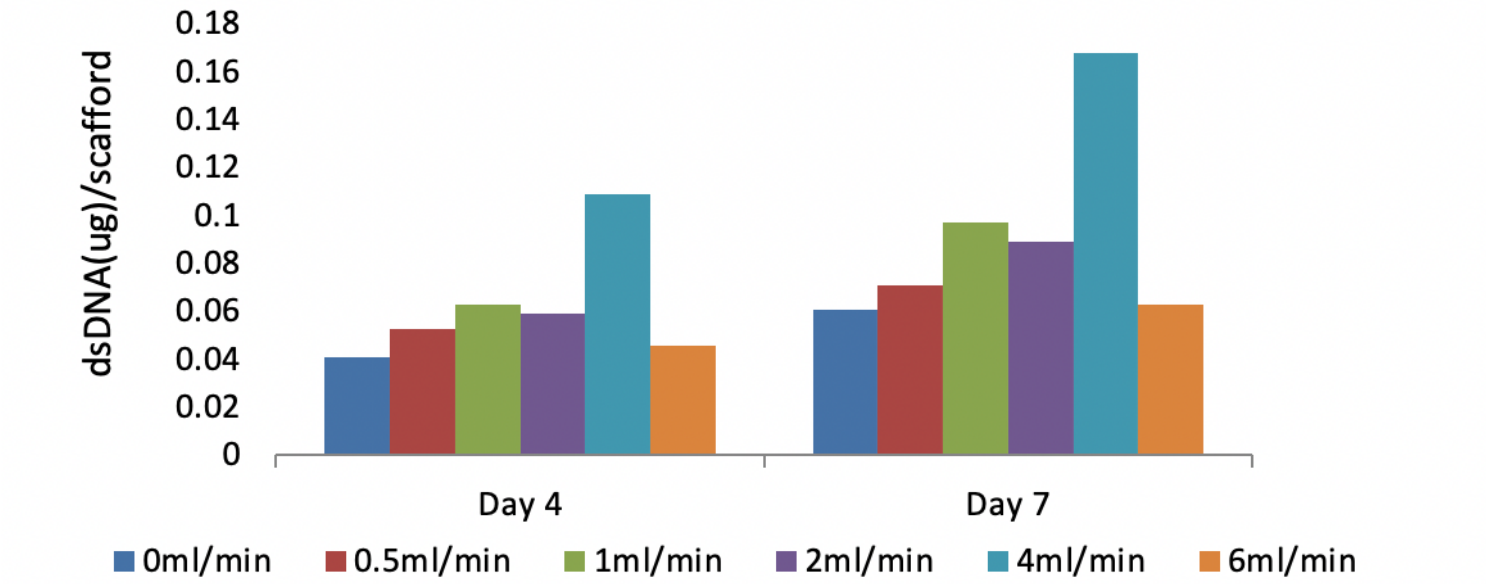


**Figure 3**

DNA quantification of BMSCs in the APB on day 4 and day 7

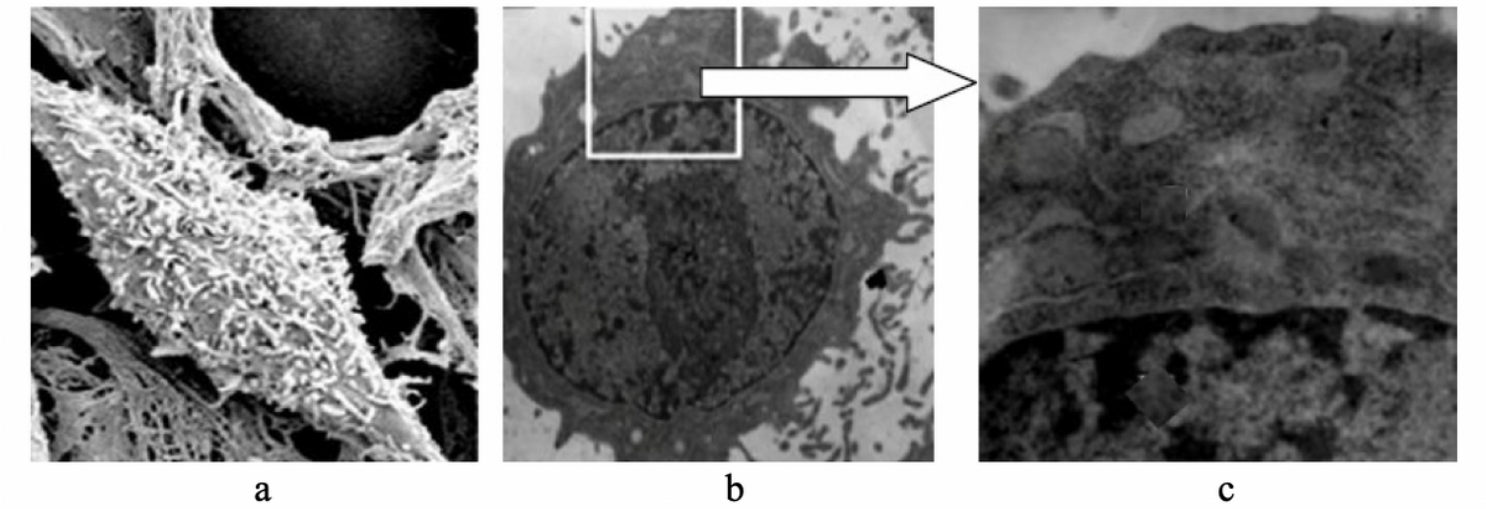


**Figure 4**

The undifferentiated BMSCs by SEM and TEM a)The undifferentiated BMSCs by SEM (Scale bars=1μm). b) (Scale bars=1μm) c) (Scale bars=300nm) Not any mature organelle by TEM.

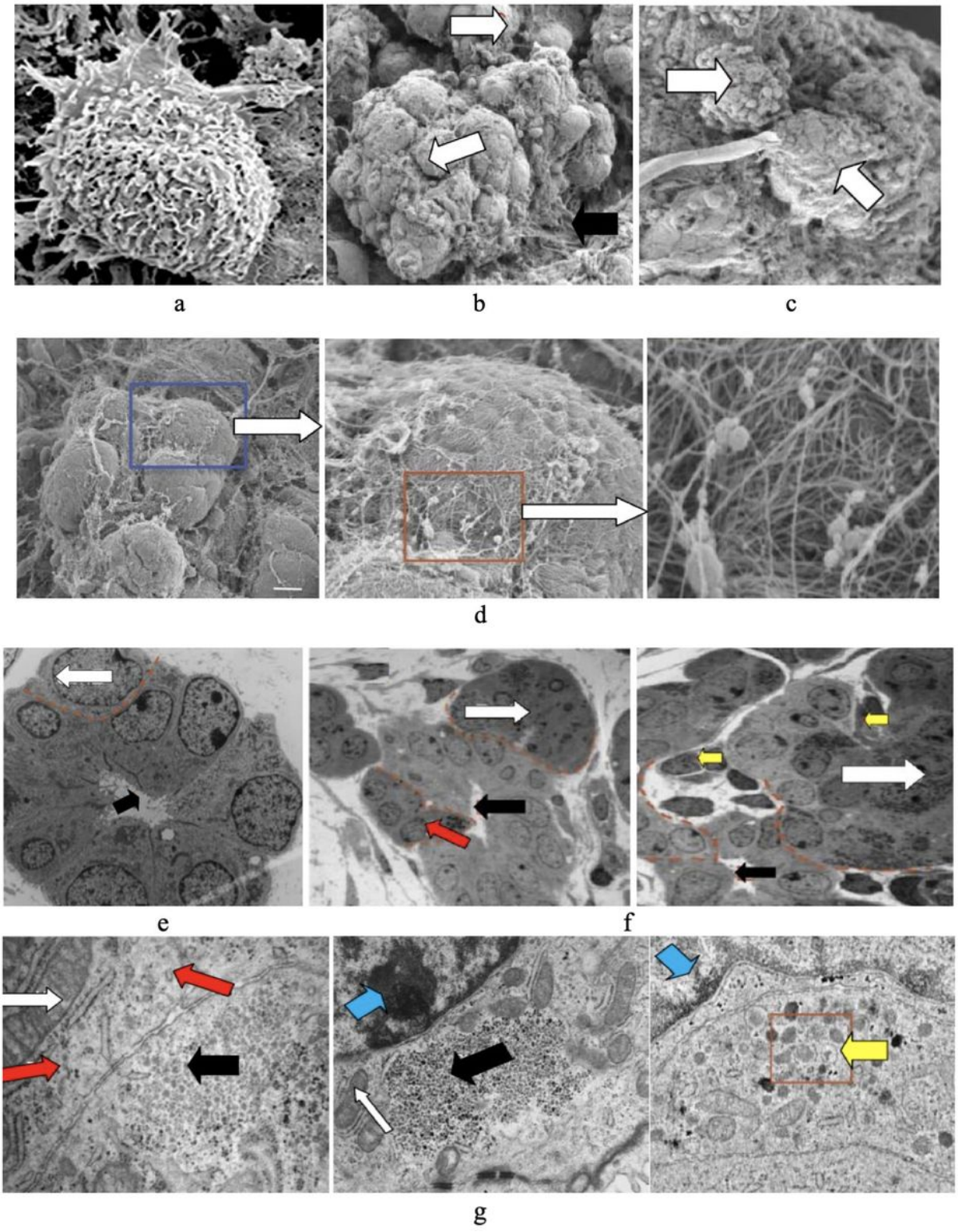


## Figure 5

The differentiated BMSCs by SEM and TEM a) The differentiated BMSCs at the 21st day by SEM (Scale bars=1μm). b) The increased number of epithelial-like cell clusters with complex intercalation of ECM (Scale bars=50μm). c) Differentiating endocrine and exocrine cells,and isolated small clusters(Scale bars=50μm). d) ECM accumulated around newly differentiated cells and clusters (Scale bars=10μm). e) Pancreatic-like epithelial cells organized into ductal structures by TEM(Scale bars=10μm). f) The

epithelial cells in clusters separate from the ducts. Acinar cells formed amylase cell clusters.The cell clusters formed islet-like structure contained capillaries(Scale bars=10μm). g) Glycogen positivity in ductal cells, nucleus, secretory granules, mitochondria, smooth endoplasmic reticulum and rough endoplasmic reticulum in differentiated BMSCs by TEM(Scale bars=1μm).

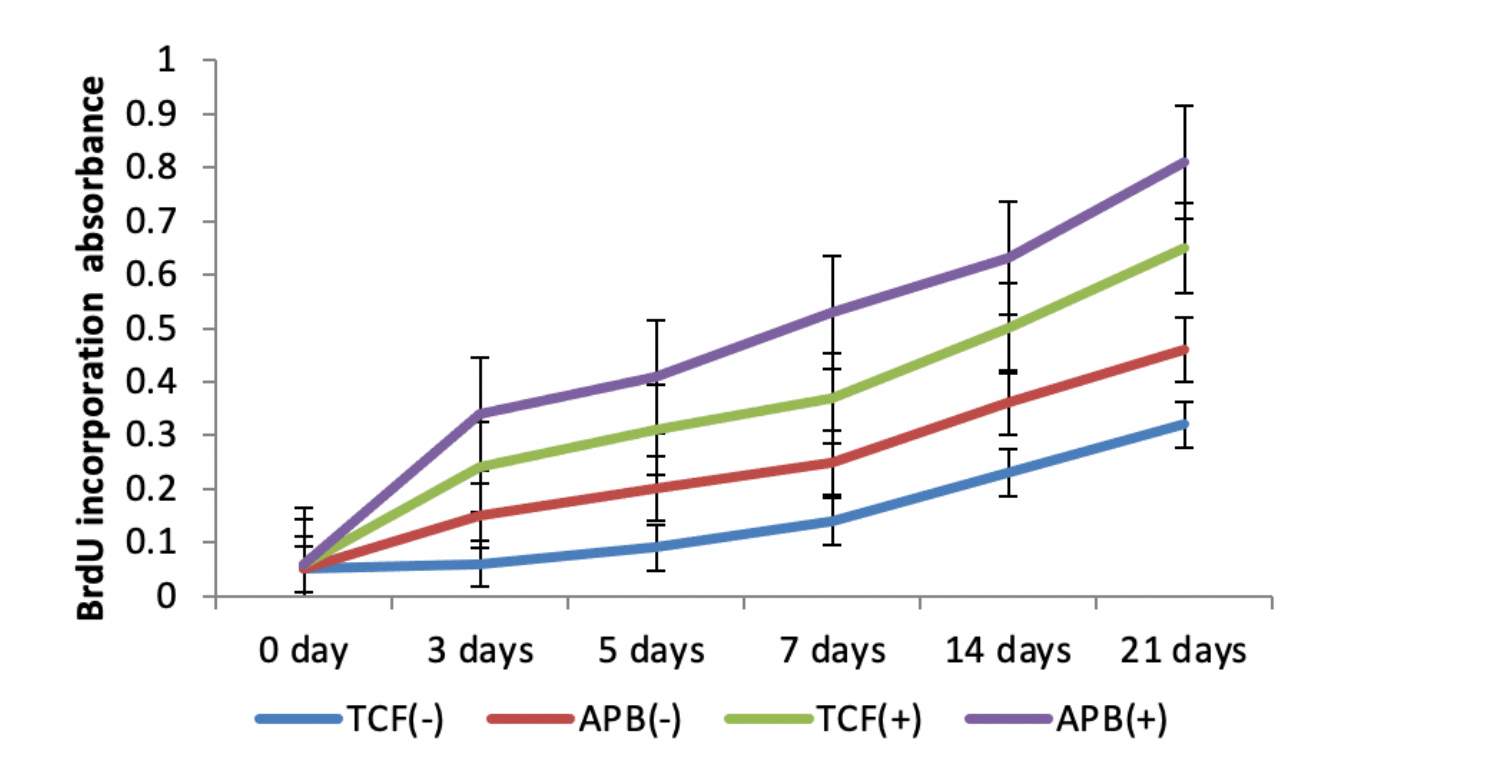


**Figure 6**

The proliferation of BMSCs grown on culture system

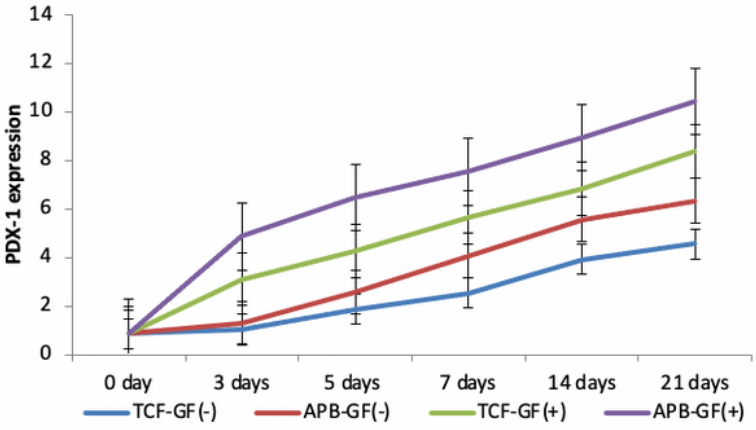


Figure 7a

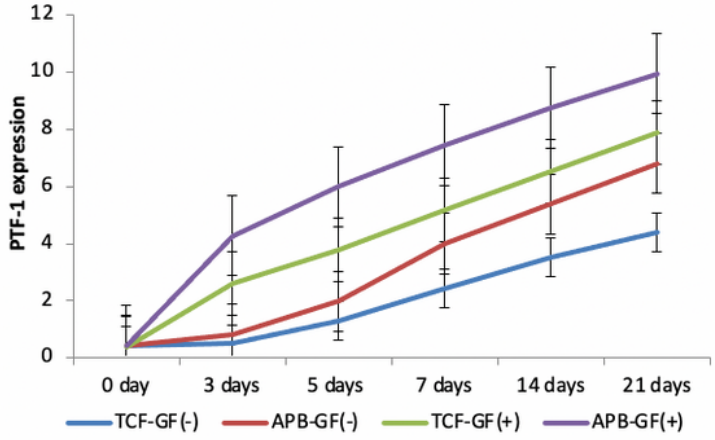


Figure 7b

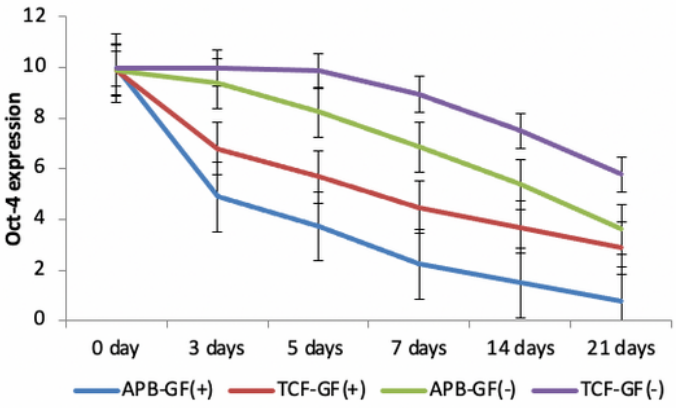


Figure 7c

## Figure 7

The expression of pancreatic and BMSCs genes a) The expression of pancreatic ancini gene PDX-1 by RT-PCR. b) The expression of pancreatic gene PTF-1 by RT-PCR. c) The expression of BMSC gene Oct4 by RT-PCR.

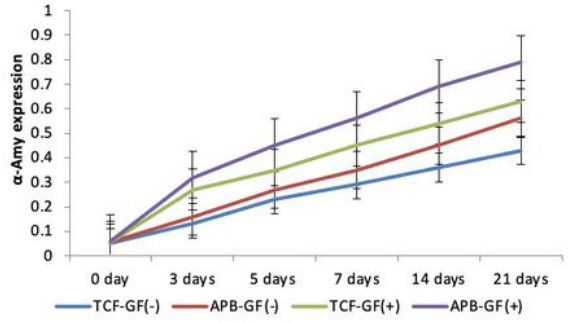


Figure 8a

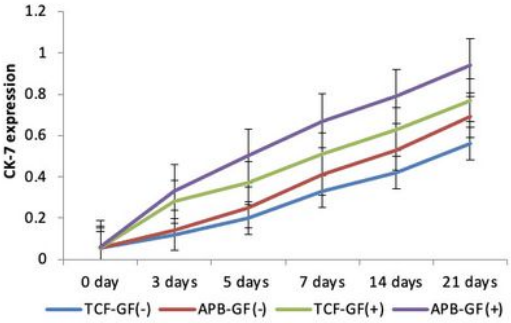


Figure 8b

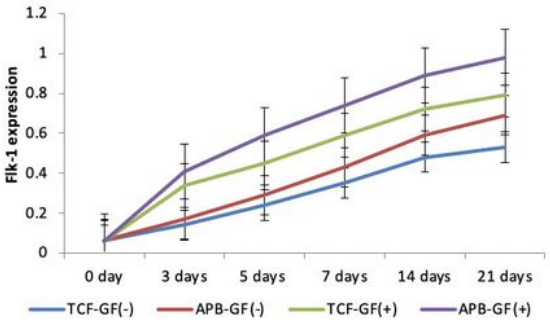


Figure 8c

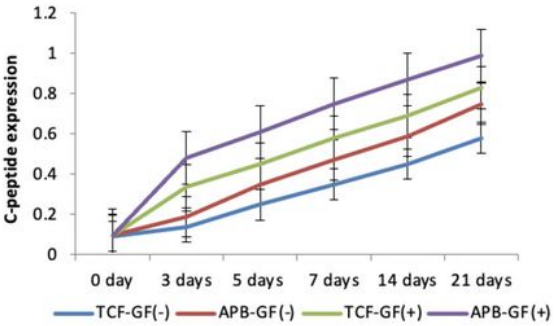


Figure 8d

## Figure 8

The expression of pancreatic cytoketatins a) The expression of pancreatic cytoketatinsα-Amy by western blot. b) The expression of pancreatic cytoketatins CK7 by western blot. c) The expression of pancreatic cytoketatins Flk-1 by western blot. d) The expression of pancreatic cytoketatins C-peptide by western blot.

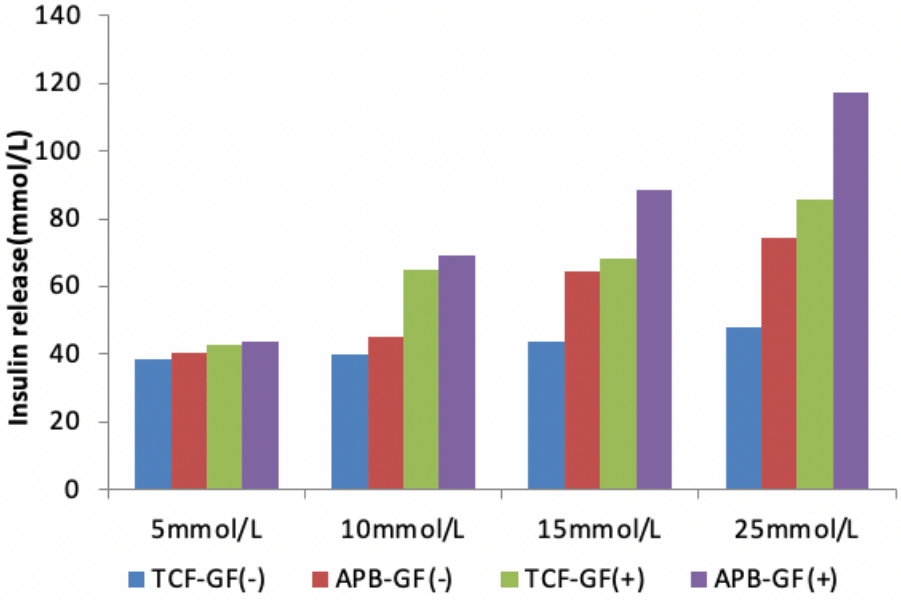


Figure 9a

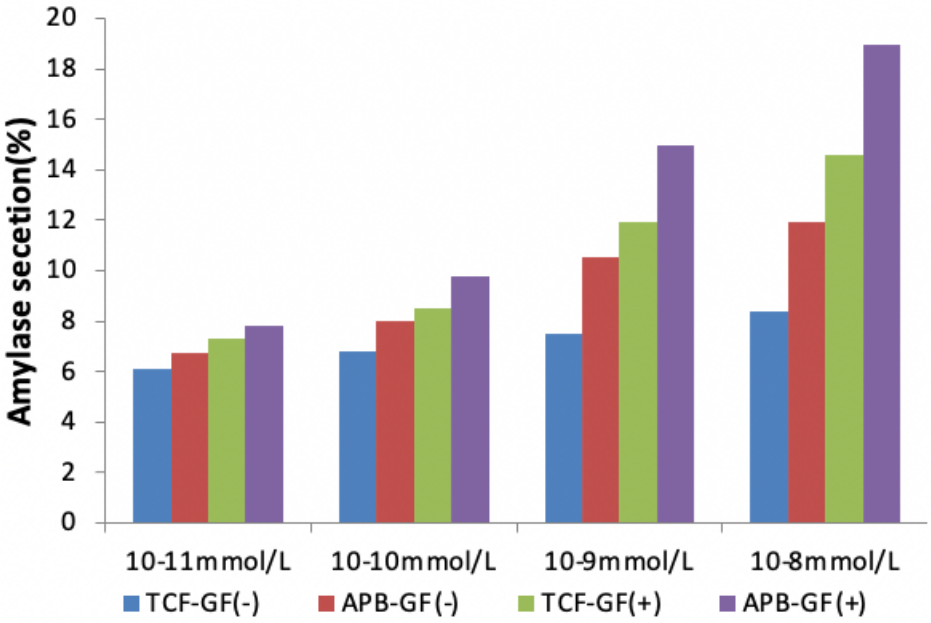


Figure 9b

## Figure 9

The assessment of pancreatic metabolic function a) The insulin release among 4 groups at increasing glucose concentrations. b) The Amylase release among 4 groups at increasing CCK concentrations.

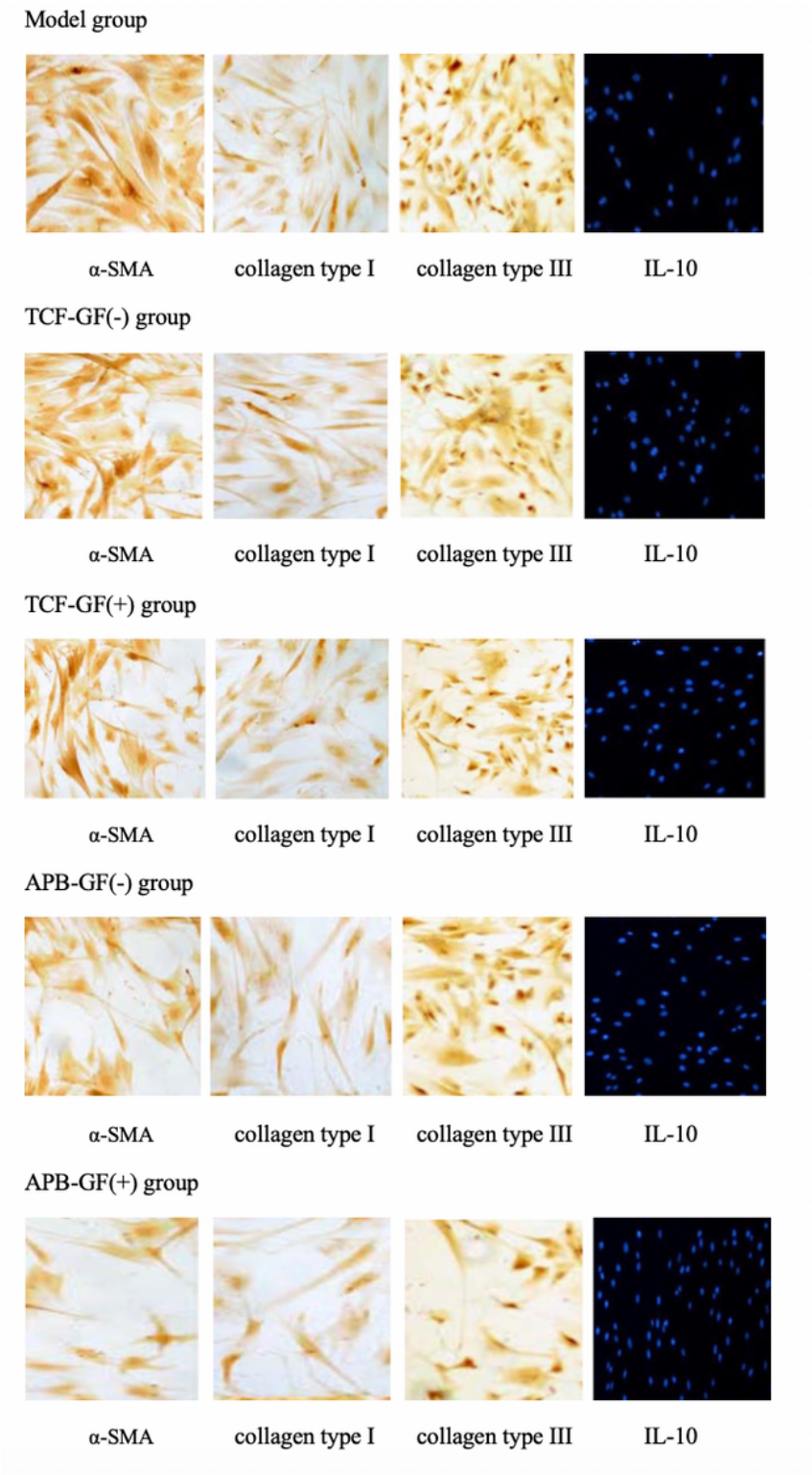


## Figure 10

The immunohistochemical evaluation of fibrotic marker levels